The EMBO Journal Vol.17 No.7 pp.1941–1951, 1998

Distinct Rab-binding domains mediate the interaction of Rabaptin-5 with GTP-bound rab4 and rab5

Gaetano Vitale, Vladimir Rybin, Savvas Christoforidis, Per-Öve Thornqvist[1], Mary McCaffrey[1], Harald Stenmark[2] and Marino Zerial[3]

European Molecular Biology Laboratory, Postfach 10.2209, D-69012 Heidelberg, Germany, [1]Department of Biochemistry, University College, Cork, Ireland and [2]Department of Biochemistry, The Norwegian Radium Hospital, Oslo, Norway

[3]Corresponding author
e-mail: zerial@embl-heidelberg.de

Rabaptin-5 functions as an effector for the small GTPase Rab5, a regulator of endocytosis and early endosome fusion. We have searched for structural determinants that confer functional specificity on Rabaptin-5. Here we report that native cytosolic Rabaptin-5 is present in a homodimeric state and dimerization depends upon the presence of its coiled-coil predicted sequences. A 73 residue C-terminal region of Rabaptin-5 is necessary and sufficient both for the interaction with Rab5 and for Rab5-dependent recruitment of the protein on early endosomes. Surprisingly, we uncovered the presence of an additional Rab-binding domain at the N-terminus of Rabaptin-5. This domain mediates the direct interaction with the GTP-bound form of Rab4, a small GTPase that has been implicated in recycling from early endosomes to the cell surface. Based on these results, we propose that Rabaptin-5 functions as a molecular linker between two sequentially acting GTPases to coordinate endocytic and recycling traffic.

Keywords: coiled coil/GTPases/Rabaptin-5/Rab5/vesicular transport

Introduction

Vesicular transport between organelles occurs with high fidelity and ensures that the biochemical composition of each intracellular compartment is accurately controlled. In order to maintain organelle homeostasis, the traffic of vesicles which fuse with a given compartment needs to be balanced with the flow of vesicles which bud from it. Early endosomes function as a primary sorting station in the endocytic pathway (Gruenberg and Maxfield, 1995; Mellman, 1996). Endocytosed molecules which enter early endosomes can be directed to the degradative pathway or be recycled back to the plasma membrane, either directly or through the perinuclear recycling endosomes (Yamashiro and Maxfield, 1984; Ghosh *et al.*, 1994; Hopkins *et al.*, 1994; Ullrich *et al.*, 1996). These processes are mediated by a continuous traffic of vesicular and tubular intermediates which needs to be coordinated to ensure proper progression of cargo through the different compartments while preserving their identity, proportions and dynamic properties.

Many molecules have been identified that function at different steps of membrane transport (Rothman, 1994). Among others, members of the Rab family of small GTPases play a central role in regulating vesicular traffic (Pfeffer, 1994; Novick and Zerial, 1997). Several Rab family members have been localized to distinct compartments of the endocytic pathway and play different roles in endocytosis and recycling (Chavrier *et al.*, 1990; van der Sluijs *et al.*, 1991; Lombardi *et al.*, 1993; Lütcke *et al.*, 1993; Olkkonen *et al.*, 1993; Ullrich *et al.*, 1996). For example, Rab5 and Rab4 both localize to early endosomes but exert opposite effects on the uptake of membrane-bound proteins such as the transferrin receptor. Overexpression of Rab5 increases the rate of fluid phase and receptor-mediated endocytosis and concomitantly induces an increase in the size of early endosomes, suggesting that this GTPase regulates the clathrin-coated pathway of receptor internalization and transport into the early endosomes (Bucci *et al.*, 1992). In contrast, cells overexpressing Rab4 exhibited normal kinetics of endocytosis but displayed a reduced uptake of fluid-phase markers and of transferrin-bound iron, and a striking accumulation of transferrin receptor on the cell surface (van der Sluijs *et al.*, 1992). In the light of these data, Rab4 has been implicated in the regulation of membrane recycling from the early endosomes to the recycling endosomes or directly to the plasma membrane (Daro *et al.*, 1996). It is not yet clear whether Rab4 and Rab5 reside on the same early endosome, or localize to distinct endosomes or subcompartments of this organelle. Nevertheless, given the complementary roles of Rab4 and Rab5 an interesting question posed by these studies is whether the two GTPases function independently or have coordinated activity.

Elucidating the functional mechanism of Rab5 and Rab4 requires the identification and molecular characterization of their regulators and effectors. To this end, we have previously identified a Rab5-interacting protein named Rabaptin-5 (Stenmark *et al.*, 1995b). Several lines of evidence indicate that Rabaptin-5 functions as an effector protein for Rab5. First, Rabaptin-5 binds directly to the GTP-bound form of Rab5 and is recruited to early endosomes by Rab5 in a GTP-dependent manner (Stenmark *et al.*, 1995b). Secondly, Rabaptin-5 stabilizes Rab5 in the GTP-bound active form by down-regulating GTP hydrolysis (Rybin *et al.*, 1996). Thirdly, its overexpression causes morphological alterations of the early endosomal compartment similar to those induced by Rab5 (Stenmark *et al.*, 1995b). Finally, it is required for the homotypic fusion between early endosomes as well as for the heterotypic fusion of clathrin-coated vesicles with early endosomes *in vitro* (Stenmark *et al.*, 1995b; Horiuchi

et al., 1997). The importance of Rabaptin-5 in endocytic transport is underlined by the finding that fragmentation of endosomes and inhibition of the endocytic pathway in apoptosis is induced by the selective cleavage and inactivation of Rabaptin-5 by proteases of the caspase family (Cosulich *et al.*, 1997). In addition, we have recently shown that cytosolic Rabaptin-5 is complexed to a 60 kDa protein, Rabex-5, which functions as a guanine-exchange factor for Rab5, suggesting that the complex couples nucleotide exchange to effector recruitment on the membrane (Horiuchi *et al.*, 1997).

In order better to understand the functional role of Rabaptin-5, we have characterized the molecule by mapping some of its structural determinants. We show that both cytosolic and recombinant Rabaptin-5 exist in a homodimeric state and that its coiled-coil predicted sequences serve as self-interacting determinants. Furthermore, we report that the Rab5-binding domain (R5BD) is located in the C-terminus of Rabaptin-5 and demonstrate that it is necessary and sufficient for Rab5-mediated recruitment of the protein on early endosomes. Unexpectedly, we identified a second Rab-binding domain (RBD) in the N-terminus of Rabaptin-5 which mediates the direct interaction with the GTP-bound, active form of Rab4. Our findings describe a novel type of structural organization for a Rab protein effector and suggest a role for Rabaptin-5 in coordinating both import to, and export from, the early endosomal compartment.

Results

N- and C-terminal coiled-coil regions mediate Rabaptin-5 homodimerization

The structural analysis of the Rabaptin-5 primary amino acid sequence by computer-assisted predictions reveals that its N- and C-terminal regions contain heptad repeats characteristic of coiled-coil domains (Stenmark *et al.*, 1995b). Two regions at the N-terminus of Rabaptin-5 (residues 12–93, CC1–1; residues 191–262, CC1–2) and two at the C-terminus (residues 551–656, CC2–1; residues 672–812, CC2–2) display the highest probability of forming coiled-coil structures (Figure 1A). Coiled-coil domains consist of seven amino acid repeats where positions one and four are predominantly non-polar and positions five and seven are mainly polar. Their overall secondary structure is α-helical and the interaction between two helices result in efficient burial of the hydrophobic side-chains at their interface.

We verified the presence of α-helices in Rabaptin-5 experimentally by analysing its overall secondary structure in aqueous solution using circular dichroism (CD) spectroscopy. Under these conditions recombinant Rabaptin-5 reveals a high content of α-helical secondary structure. The helical population calculated by the method of Cheng *et al.* (1974) from the ellipticity value at 222 nm is ~70% (Figure 2A). This confirms that the overall Rabaptin-5 secondary structure is compatible with the presence of large coiled-coil domains.

Given that proteins such as myosins (Harrington and Rodgers, 1984) and lamins (Heitlinger *et al.*, 1991) form stable homodimers through their coiled-coil domains, we used chemical cross-linking to test the ability of cytosolic Rabaptin-5 to dimerize. Upon Bis(Sulfosuccinimidyl) suberate (BS^3) cross-linking, SDS–PAGE and immunoblot analysis (Figure 2B) a major cross-linked product of Rabaptin-5 from cytosol migrated at the apparent M_r of ~200 kDa, as expected for a homodimer. Cross-linking of Rabaptin-5 dimers was titratable and quantitative up to 1.5 mM BS^3. A band of similar size was also detected with purified recombinant Rabaptin-5, indicating that both the recombinant and the cytosolic protein exist in a dimeric state. At the highest concentration of cross-linking reagent a number of bands at molecular mass >200 kDa appeared both with cytosolic and recombinant Rabaptin-5. These bands may correspond to inter- and intra-molecular cross-linked products.

The existence of Rabaptin-5 homodimers was confirmed by fractionating bovine brain cytosol and recombinant Rabaptin-5 using a combination of sedimentation on a linear glycerol gradient and gel-filtration chromatography on a Superose-6 column. From the estimated Stokes radius R_s = 12 nm and $S_{20,w}$ = 6.5 we have previously calculated the M_r of cytosolic Rabaptin-5 to be ~330 kDa (Horiuchi *et al.*, 1997). Using the same approach we estimated the Stokes radius R_s = 9 nm and $S_{20,w}$ = 4.8 for recombinant Rabaptin-5 alone, corresponding to a M_r of ~200 kDa, consistent with the formation of homodimers. The difference between the molecular mass of cytosolic and recombinant Rabaptin-5 is in agreement with the fact that *in vivo*, Rabaptin-5 is complexed to other cytosolic proteins such as Rabex-5 and p50 (Horiuchi *et al.*, 1997). Thus, the hydrodynamic properties we measured provide further support for the homodimerization of Rabaptin-5.

To test the role of the individual predicted coiled-coil sequences in Rabaptin-5 dimerization, we made use of the yeast two-hybrid system. We cloned Rabaptin-5 full-length cDNA as well as the four putative coiled-coil sequences (CC) in both 'bait' (as C-terminal fusion with the LexA DNA-binding domain) and 'prey' (as C-terminal fusion with the Gal4 activation domain) two-hybrid vectors and transformed them in the yeast reporter strain L40. As a control for specificity we used a LexA fusion bait with the Coil1B domain of lamin C (McKeon *et al.*, 1986). The *trans*-activation of the *HIS3* reporter upon bait–prey interaction was revealed by the ability of the yeast transformants to grow on histidine-lacking medium. As shown in Figure 3A, Rabaptin-5 interacts with itself but not with the Coil1B domain of laminC. The individual CC sequences could interact both with full-length Rabaptin-5 (Figure 3A) and with themselves (Figure 3C), whereas no interaction was detected with the Coil1B domain of lamin C (Figure 3A). These results confirm that Rabaptin-5 can homodimerize and further indicate that the predicted CC sequences function as self-interacting determinants.

73 amino acid residues in Rabaptin-5 are necessary and sufficient for interaction with Rab5 and for Rab5-dependent recruitment on early endosomes

Rabaptin-5 was originally identified in a two-hybrid screen as clone L1_46, which encodes the C-terminus of the molecule (amino acids 551–862) and is responsible for the interaction with GTP-bound Rab5 (Stenmark *et al.*, 1995b). In order to gain more information about this interaction, we mapped the sequence within the C-terminus of Rabaptin-5, which interacts with Rab5. By

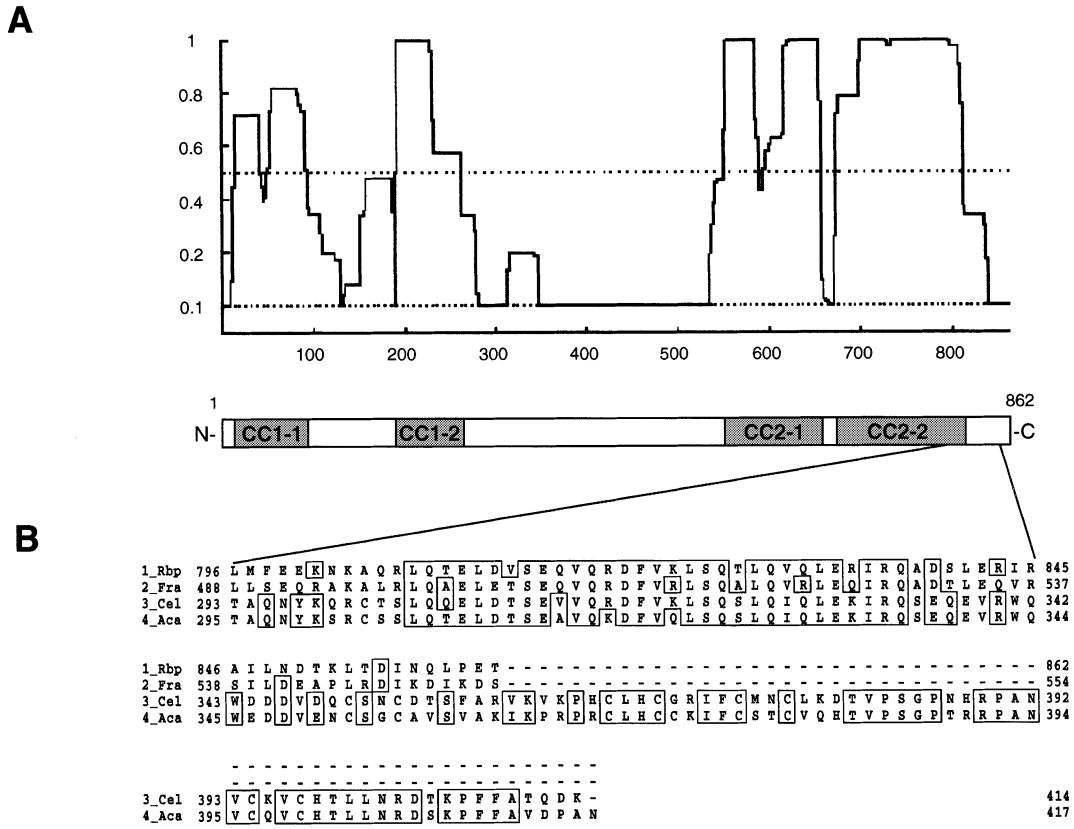

Fig. 1. (**A**) Schematic organization of the putative coiled-coil sequences of Rabaptin-5, and (**B**) sequence alignment between Rabaptin-5 and three related protein sequences at their respective C-termini. (A) Histogram indicating the probability of forming α-helical coiled-coil structures in Rabaptin-5 as determined using the Paircoil program (Berger *et al.*, 1995). The *y*-axis shows the predicted probability (0–1 represents 0–100%) of α-helical coiled-coil formation, while the *x*-axis indicates the amino acid number for Rabaptin-5. Rabaptin-5 regions with a predicted probability >50% of forming coiled-coil structures are indicated as grey areas in the scheme below the histogram. (B) Alignment of Rabaptin-5 (1_Rbp), with the protein translations of the DDBJ/EMBL/GenBank database sequences U34932 (2_Fra), U13070 (3_Cel), and U17585 (4_Aca) at their respective C-termini. The sequence alignment was performed with the program PileUp, and displayed with the PrettyPlot program of the GCG package. Numbers represent amino acid positions.

databank homology searches, we found that Rabaptin-5 shares homology with three sequences, one from rat and two from the nematodes *Caenorhabditis elegans* and *Angiostrongylus cantonensis* (Figure 1B), with a pronounced degree of identity (~75%) at their respective C-termini (residues 780–836 for Rabaptin-5). The rat sequence corresponds to a Rabaptin-5-like molecule that has been independently identified as a Rab5-interacting protein (Horiuchi *et al.*, 1997; Gournier *et al.*, 1998). The *C.elegans* open reading frame has not been characterized so far, while the sequence from *A.cantonensis* encodes a muscle-associated protein specifically expressed in adult female worms (Joshua and Hsieh, 1995). The high sequence conservation of this region and its position in the C-terminus of Rabaptin-5 made it a candidate for a R5BD.

To test this possibility, we analysed a series of N-terminal L1_46 deletion mutants (Figure 4a), both in the two-hybrid system for their ability to interact with the GTPase-deficient Rab5^{Q79L} mutant and for recruitment on early endosomes as C-terminal fusions with a cytosolic reporter, the Green-Fluorescent protein (GFP) of *Acquorea victoria*. By the yeast two-hybrid system, we detected interaction between Rab5^{Q79L} and a C-terminal fragment of Rabaptin-5 corresponding to residues 789–862 (Figure 4a). A deletion within this sequence (L1_46 Δ809–832) abolished the interaction, indicating that this region contains structural elements which are necessary for the association with Rab5. We confirmed this interaction by fluorescence microscopy in HeLa cells co-expressing Rab5^{Q79L} and fusions between GFP and Rabaptin-5 C-terminal sequences. GFP alone gave a diffuse cytosolic localization when co-expressed with Rab5^{Q79L} (Figure 4b, panel A). In contrast, GFP localized on enlarged early endosomes induced by the expression of the Rab5 mutant when fused to the L1_46 protein (Figure 4b, panel B). Among the L1_46 deletions tested (Figure 4b, panels C–F), the Rabaptin-5 789–862 mutant, which could interact with Rab5^{Q79L} in the yeast two-hybrid system (Figure 4a), was also recruited on early endosomes (Figure 4b, panel E). Interestingly, a further deletion of the 30 most C-terminal amino acids (Rabaptin-5 789–832) did not impair membrane association. Although the region comprising residues 789–832 did not support interaction in the yeast two-hybrid system (Figure 4a), it appears that this fragment nevertheless allows recruitment on endosomal membranes *in vivo*. All GFP fusion proteins showed diffuse cytosolic staining when expressed alone (not shown). Altogether, the combination of yeast two-hybrid system and fluorescence microscopy data indicates that the R5BD lies within a 73 amino acid sequence in the C-terminus of Rabaptin-

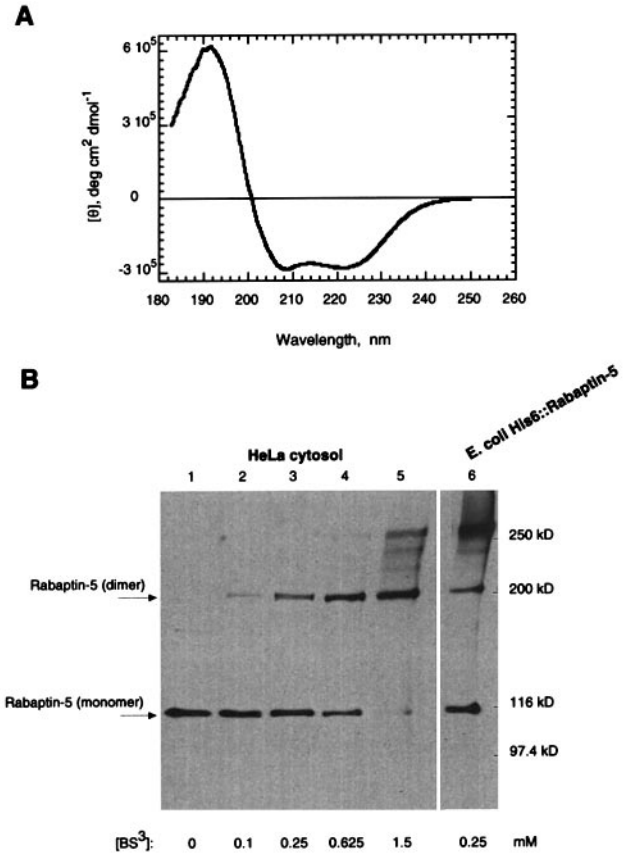

Fig. 2. (**A**) CD analysis of recombinant His_6::Rabaptin-5, and (**B**) SDS–PAGE electrophoresis and anti-Rabaptin-5 immunoblot of cross-linked products from cytosol and recombinant His_6::Rabaptin-5. (A) CD spectrum was recorded from 1 μM His_6::Rabaptin-5, 10 mM phosphate-buffered solution (pH 7.2) in the presence of 0.5 mM 2-mercaptoethanol; the *y*-axis shows the ellipticity value θ (expressed in deg cm^2/dmol), while the *x*-axis indicates wavelength (in nm). (B) 20 μg of HeLa cytosol (lanes 1–5) and 40 ng of recombinant His_6::Rabaptin-5 (lane 6) were incubated with the indicated concentrations of the covalent cross-linker BS^3 and subsequently analysed by SDS–PAGE followed by immunoblotting using affinity-purified anti-Rabaptin-5 antibodies.

5. This region is conserved among other Rabaptin-like proteins from rat and nematodes, and is sufficient for Rab5-dependent recruitment of the protein on early endosomal membranes.

Rab4 interacts with Rabaptin-5 via a distinct RBD

Next we tested whether the C-terminal R5BD is the only RBD present in Rabaptin-5. The interaction specificity of the L1_46 protein was previously analysed with a panel of different Rab baits and found to be highly specific for Rab5 (Figure 5A; Stenmark *et al.*, 1995b). Surprisingly, when we extended this analysis to full-length Rabaptin-5 as prey (Figure 5B), we found that the protein strongly interacts with $Rab5^{Q79L}$ but also with the GTPase-deficient $Rab4^{Q67L}$ mutant. Importantly, besides a weak interaction with Rab3a (the significance of which is not clear at the moment), full-length Rabaptin-5 failed to interact with other Rab proteins of the endocytic or biosynthetic pathway (Rab6, Rab7, Rab17 and Rab22; also see below) indicating that Rabaptin-5 does not interact indiscriminately with all family members.

The observation that Rabaptin-5 interacts with Rab4 and Rab5 is intriguing in the light of previous studies showing that both GTPases reside on early endosomes (Chavrier *et al.*, 1990; van der Sluijs *et al.*, 1992). We therefore investigated this interaction further and mapped the Rab4-binding domain (R4BD). The yeast two-hybrid analysis indicated that the deletion mutant Rabaptin-5 551–862 failed to interact with $Rab4^{Q67L}$ (Figure 5A). Conversely, an N-terminal prey construct (amino acids 5–547) tested against the same panel of Rab baits showed an efficient interaction with Rab4 but a very weak or undetectable association with Rab5 and other Rab proteins (Figure 5C; see below). It thus appears that the sequences interacting with Rab4 and Rab5 are located in topologically distinct regions of Rabaptin-5, i.e. in the N- and C-terminus, respectively. In order to map more precisely the localization of the R4BD, we tested several Rabaptin-5 C-terminal deletions in the two-hybrid system for their ability to interact with $Rab4^{Q67L}$. As shown in Figure 6A, a Rabaptin-5 fragment corresponding to amino acids 5–135 retained the ability to interact with $Rab4^{Q67L}$. Interestingly, this region does not share significant sequence homology with the region harbouring the R5BD.

To confirm that Rabaptin-5 can bind Rab4 in a nucleotide-dependent manner, a Rab4 N-terminal fusion with maltose-binding protein (MBP::Rab4) was covalently bound on Affi-Gel 15 beads, pre-loaded with GDP or GTPγS, or in a nucleotide-free state, and assayed for binding of recombinant (Figure 6B, upper panel) or cytosolic Rabaptin-5 (Figure 6B, lower panel). In both cases Rabaptin-5 interacted with MBP::Rab4 loaded with GTPγS. Consistent with the two-hybrid analysis shown in Figure 5, only background levels of Rabaptin-5 binding were detected with GDP-loaded MBP::Rab4 or in the absence of nucleotide, or with an MBP::Rab6 fusion, indicating that the interaction with Rab4 is specific and depends on the GTP-bound conformation.

Independent biochemical evidence that Rabaptin-5 can interact with both Rab5 and Rab4 in a GTP-dependent manner was obtained by gel-filtration chromatography. Rab5 and Rab4 were pre-loaded with either GDP or GTPγS and then incubated in the presence of recombinant Rabaptin-5. The proteins were fractionated on a Superdex-200 column and analysed by SDS–PAGE and Western blot. The position of Rabaptin-5 on the chromatogram was consistent with the M_r corresponding to the homodimer. As shown in Figure 6C, the fractions corresponding to the Rabaptin-5 homodimer peak also contained both Rab5 and Rab4 pre-loaded with GTPγS. However, no cofractionation was detected when the proteins were pre-loaded with GDP (data not shown).

Finally, we examined the subcellular localization of Rab4 and Rabaptin-5 by confocal immunofluorescence microscopy. Since the available antibodies against Rab4 failed to detect endogenous levels of the protein, we co-expressed VSV-G tagged $Rab4^{Q67L}$ or $Rab5^{Q79L}$ with either full-length *myc*-tagged Rabaptin-5 or various N- and C-terminal deletions in BHK cells, using the T7 RNA polymerase recombinant Vaccinia virus system. As shown in Figure 7A, VSV-G::$Rab4^{Q67L}$ localized to vesicular structures dispersed throughout the cytoplasm which were also labelled for the human transferrin receptor (hTfR), in agreement with previous studies (van der Sluijs *et al.*, 1991; Daro *et al.*, 1996). However, when VSV-

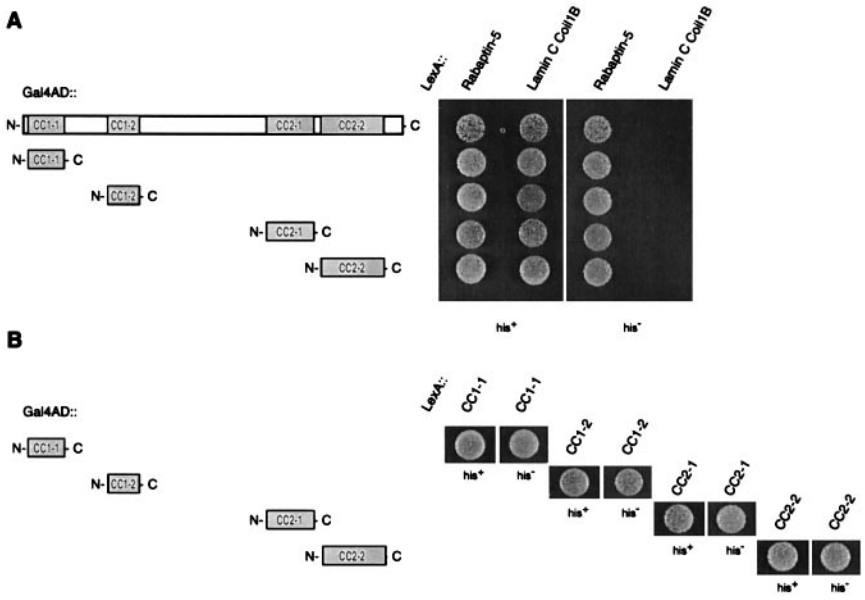

Fig. 3. Identification of Rabaptin-5 self-interacting determinants by the yeast two-hybrid system. *HIS3* reporter gene activation caused by specific interactions between various bait and prey Rabaptin-5 fusions in the two-hybrid system. L40 reporter yeast cells co-transformed with Gal4 RNA polymerase II activation domain (Gal4AD::) fusions in the 2μ/LEU2 pGAD10 plasmid and LexA DNA-binding domain fusions in the 2μ/TRP1 pLexA plasmid (LexA::) of the proteins indicated were spotted on synthetic complete medium lacking tryptophan and leucine (his^+) or lacking tryptophan, leucine and histidine (his^-). (**A**) Rabaptin-5 self-interaction and interaction between the full-length molecule and the four individual coiled-coil predicted sequences; a LexA bait fusion (LexA::) with the Coil1B domain of laminC was used as control for non specific coiled-coil interactions. (**B**) Self-interaction between the individual coiled-coil predicted sequences.

G::$Rab4^{Q67L}$ was co-expressed with *myc*::Rabaptin-5 the two proteins accumulated on enlarged endosomes whose expansion is caused by the overexpression of Rabaptin-5 alone (Figure 7B; Stenmark *et al.*, 1995b). Thus, as predicted on the basis of their interaction, Rabaptin-5 and VSV-G::$Rab4^{Q67L}$ co-localize to the same endosomal compartment. If Rabaptin-5 can bind both Rab5 and Rab4 on the same endosome the two Rab proteins would be expected to co-localize substantially upon overexpression of Rabaptin-5. Indeed, Figure 7C shows that while structures containing predominantly Rab5 or Rab4 proteins are visible, the large endosomes induced by the overexpression of Rabaptin-5 contain both VSV-G::$Rab4^{Q67L}$ and endogenous Rab5. Moreover, when co-expressed, VSV-G::$Rab4^{Q67L}$ and *myc*:: $Rab5^{Q79L}$ were also found to co-localize to enlarged endosomal structures (Figure 7E). As control, Rab7 (a late endosomal-specific small GTPase) and *myc*::Rabaptin-5 were clearly found segregated in different compartments (Figure 7D). We did not observe membrane recruitment of two Rabaptin-5 C-terminal deletions (*myc*::Rabaptin-5 Δ547–862, Figure 7F; and *myc*::Rabaptin-5 Δ215–862, data not shown) by VSV-G::$Rab4^{Q67L}$ despite the presence of the R4BD. These results suggest that the interaction between Rab4 and the R4BD on the membrane is either not stable or it requires the full-length molecule (see Discussion). Conversely, VSV-G::$Rab5^{Q79L}$ was able to recruit the C-terminal region of Rabaptin-5 containing the R5BD (*myc*::Rabaptin-5 with the N-terminal Δ1–550 deletion; Figure 7G) on endosome membranes, but not the N-terminus containing the R4BD (*myc*::Rabaptin-5 Δ551–862; Figure 7H). These data provide further support for the conclusion that the membrane recruitment of Rabaptin-5 by Rab5 is mediated by the C-terminally located R5BD.

Discussion

We have previously identified a Rab5 effector protein, Rabaptin-5, which specifically interacts with Rab5 in the GTP-bound conformation and is required for Rab5-dependent early endosome fusion (Stenmark *et al.*, 1995b). Here we report the characterization of several Rabaptin-5 structural determinants. We found that Rabaptin-5 dimerizes through N- and C-terminal sequences predicted to form coiled-coil structures. A conserved 73 amino acid C-terminal sequence is necessary and sufficient for Rab5 interaction and Rab5-mediated membrane recruitment of Rabaptin-5. A surprising outcome of our analysis is the identification of a second RBD which is located in the N-terminus of Rabaptin-5 and mediates the direct interaction with GTP-bound Rab4. Given that like Rab5, Rab4 is localized to early endosomes but is implicated in the regulation of recycling, our results have important implications concerning the role of Rabaptin-5 in coordinating endocytosis and recycling.

Coiled-coil domains are protein–protein interaction determinants (Lupas, 1996) which are found in components of the membrane transport machinery such as v- and t-SNAREs, the integral membrane proteins that are thought to mediate the formation of the docking–fusion complex (Rothman, 1994). We observed that Rabaptin-5 exhibits a high content of α-helical secondary structure and exists in a homodimeric state in cytosol, and that its coiled-coil predicted structures are used as self-interacting determinants. The dimeric coiled-coil structures may provide a backbone for the assembly of a multi-protein complex, given that Rabaptin-5 interacts with at least two other molecules in cytosol, Rabex-5 and an as yet uncharacterized p50 (Horiuchi *et al.*, 1997). Dimerization of Rabaptin-5 could also form a divalent

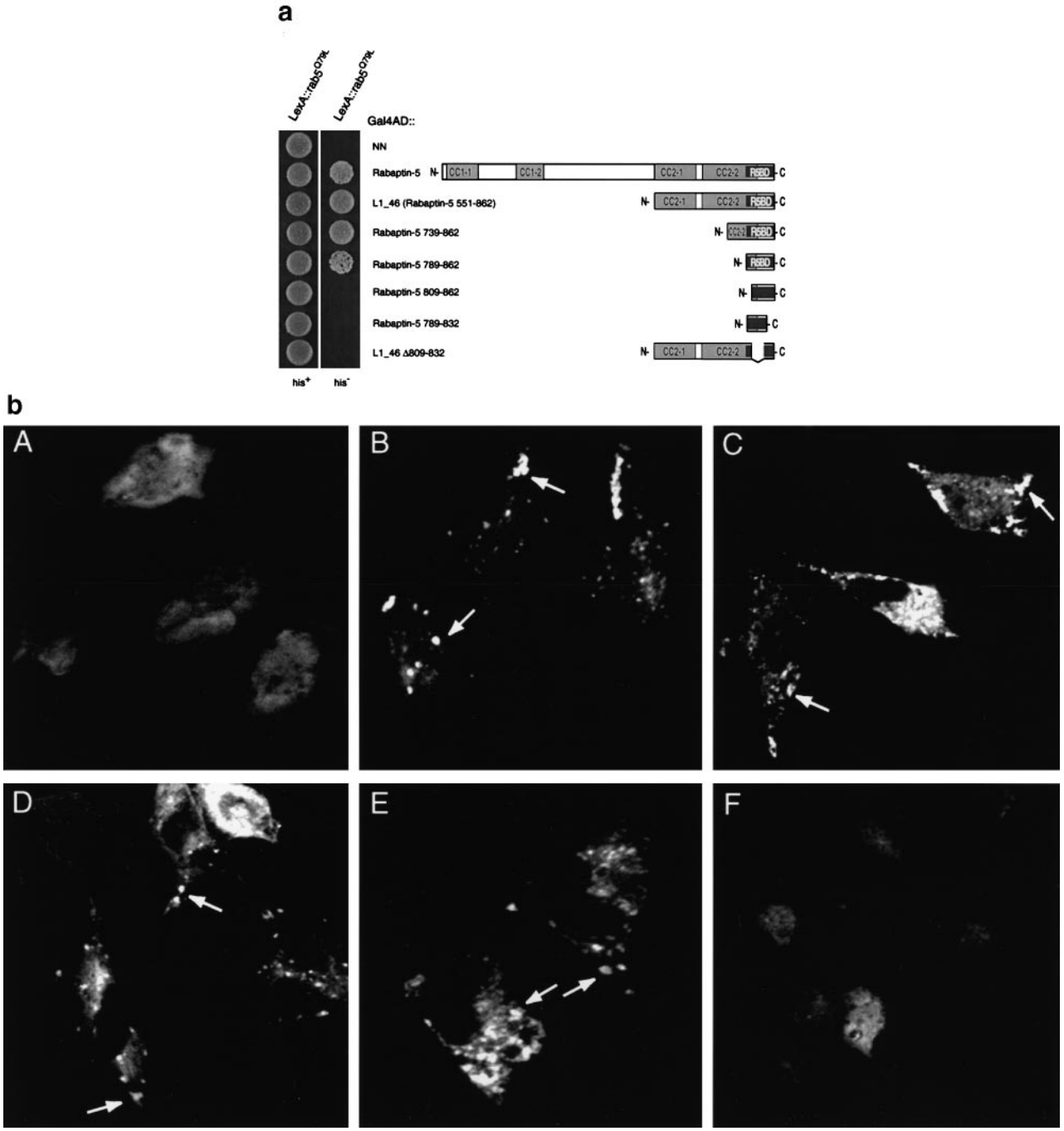

Fig. 4. (**a**) Mapping of the R5BD of Rabaptin-5 by the yeast two-hybrid system, and (**b**) confocal fluorescence microscopy of cells co-expressing $Rab5^{Q79L}$ and GFP or GFP::Rabaptin-5 fusions. (A) *HIS3* reporter gene activation caused by specific interactions between the indicated Rabaptin-5 deletions Gal4AD fusions in pGADGH and LexA::$Rab5^{Q79L}$, tested as growth in synthetic medium lacking tryptophan, leucine and histidine (his^-). (b) BHK cells infected with T7 RNA polymerase recombinant vaccinia virus (vT7), were co-transfected with $Rab5^{Q79L}$ (panels A–F), and: (panel A) the Green Fluorescent protein (GFP); (panel B) GFP::Rabaptin-5 551–862; (panel C) GFP::Rabaptin-5 739–862; (panel D) GFP::Rabaptin-5 789–862; (panel E) GFP::Rabaptin-5 789–832; or (panel F) GFP::Rabaptin-5 807–862. The cells plated on 11 mm glass coverslips were infected and transfected for 3.5 h as described previously (Stenmark *et al.*, 1994b), incubated at 30°C for 30 min, fixed and viewed with the confocal microscope developed at EMBL, also as described previously (Bucci *et al.*, 1992). Arrows indicate typical membrane structures formed upon $Rab5^{Q79L}$ expression and decorated (panels B–E) with the GFP::Rabaptin-5 fusion proteins.

Rab5-binding site, since single Rabaptin-5 chains can bind Rab5 (Horiuchi *et al.*, 1997). In this case, the nucleotide-exchange activity of Rabex-5 in the Rabaptin-5 complex could engage two Rab5 molecules to bind simultaneously the Rabaptin-5 homodimer on the membrane. Upon membrane recruitment by Rab5–GTP, Rabex-5 would convert a second Rab5 molecule into the GTP-bound form to bind the second Rabaptin-5 chain of the dimer, thus increasing the stability of association with the membrane. As a dimer, Rabaptin-5 would also be expected to reside longer on the membrane, as two Rab5 molecules would have to hydrolyse GTP in order to release Rabaptin-5 in the cytosol.

The C-terminal 73 amino acid sequence of Rabaptin-5

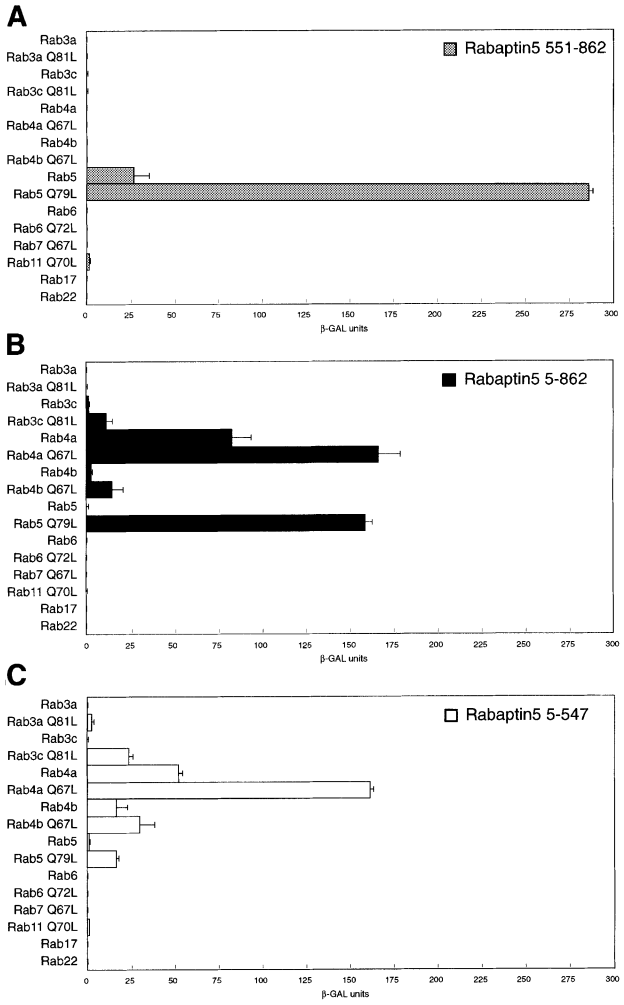

Fig. 5. Interaction specificity of Rabaptin-5 and C- or N-terminal deletions with Rab family members in the yeast two-hybrid system. Interaction between Rabaptin-5 (**A**) C-terminal, (**B**) full-length or (**C**) N-terminal Gal4BD prey fusions in pGADGH, and various bait LexA::Rab fusions assayed as *lacZ* reporter gene activity in liquid β-Gal assay. L40 reporter yeast cells transformed with the 2μ/TRP1 pLexA plasmids encoding for the indicated LexA::Rab fusion and with 2μ/LEU2 pGADGH plasmids encoding Gal4 fusions of Rabaptin-5 and the C- or N-terminal deletions, were grown to OD_{600} values of ~1.0 in synthetic medium lacking tryptophan and/or leucine. β-galactosidase (β-Gal) activity was then measured, using *O*-nitrophenyl-β-D-galactoside (Sigma) as a substrate (Guarente, 1983). β-Gal activities (in relative units) are presented in boxes as mean values ±SEM (bars) obtained with three independent transformants.

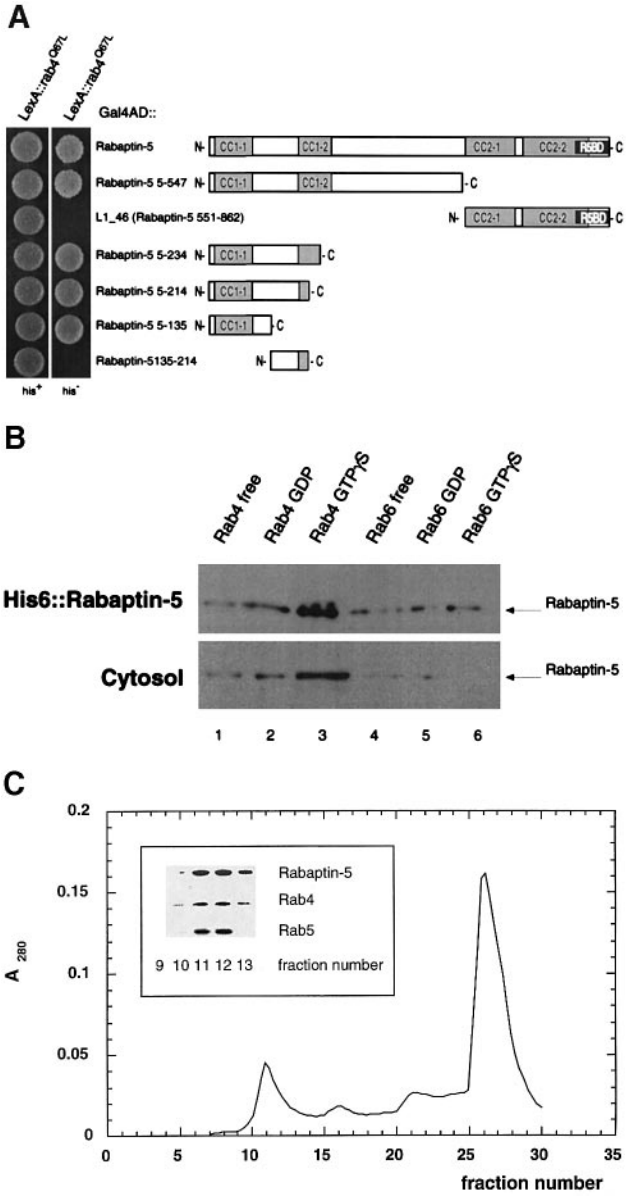

Fig. 6. (**A**) Mapping of the R4BD of Rabaptin-5 by the yeast two-hybrid system, (**B**) *in vitro* binding of cytosolic or recombinant His_6::Rabaptin-5 to MBP::Rab4 and (**C**) cofractionation of Rab4, Rab5 and Rabaptin-5 by size exclusion chromatography. (A) *HIS3* reporter gene activation caused by specific interactions between various indicated Rabaptin-5 deletions, Gal4AD fusions and LexA::$Rab4^{Q67L}$, tested as growth in synthetic medium lacking tryptophan, leucine and histidine (his^-). (B) Aliquots of Affi-Gel 15 beads containing immobilized MBP::Rab4 or MBP::Rab6 pre-loaded with 100 μM GDP (lanes 2 and 5), GTPγS (lanes 3 and 6) or buffer alone (free form, lanes 1 and 4) were incubated in the presence of 5 μg His_6::Rabaptin-5 or with 200 μg of bovine brain cytosol. After washing, Rabaptin-5 associated with the beads was detected by SDS–PAGE followed by immunoblotting. (C) Following pre-loading with GTPγS, recombinant His-Rab4 and His-Rab5 were incubated with Rabaptin-5 and the reaction mixture was separated on a Superdex-200 column. Proteins in the fractions were detected by measuring absorbance at 280 nm and Western blot analysis (inset for fractions 9–13) using anti-Rabaptin-5, -Rab4 and -Rab5 rabbit polyclonal antibodies. The peak of A_{280} in fractions 25–30 corresponds to a M_r of 25–27 kDa and contains the excess of free GTPases.

shares high sequence homology with the C-terminus of a Rabaptin-5-like protein that we have independently identified as a Rab5-interacting molecule (Horiuchi *et al.*, 1997; Gournier *et al.*, 1998). Our deletion mutants analysis revealed that this conserved sequence is not the only Rab-interacting site of the molecule. Rabaptin-5 specifically interacts via a distinct, structurally unrelated N-terminal RBD with GTP-bound Rab4. Although it localizes with Rab5 to the same compartment, Rab4 has been shown to play a role in recycling through the early endosomes (van der Sluijs *et al.*, 1991, 1992). It is interesting to note that Rabaptin-5 does not appear to interact (in the yeast two-hybrid system) with Rab11, a GTPase that is highly enriched on the recycling endosome and whose activity is required for receptor recycling through this compartment (Ullrich *et al.*, 1996). Thus our results suggest that two Rab proteins which act sequentially in transport through the early endosomes share the same effector.

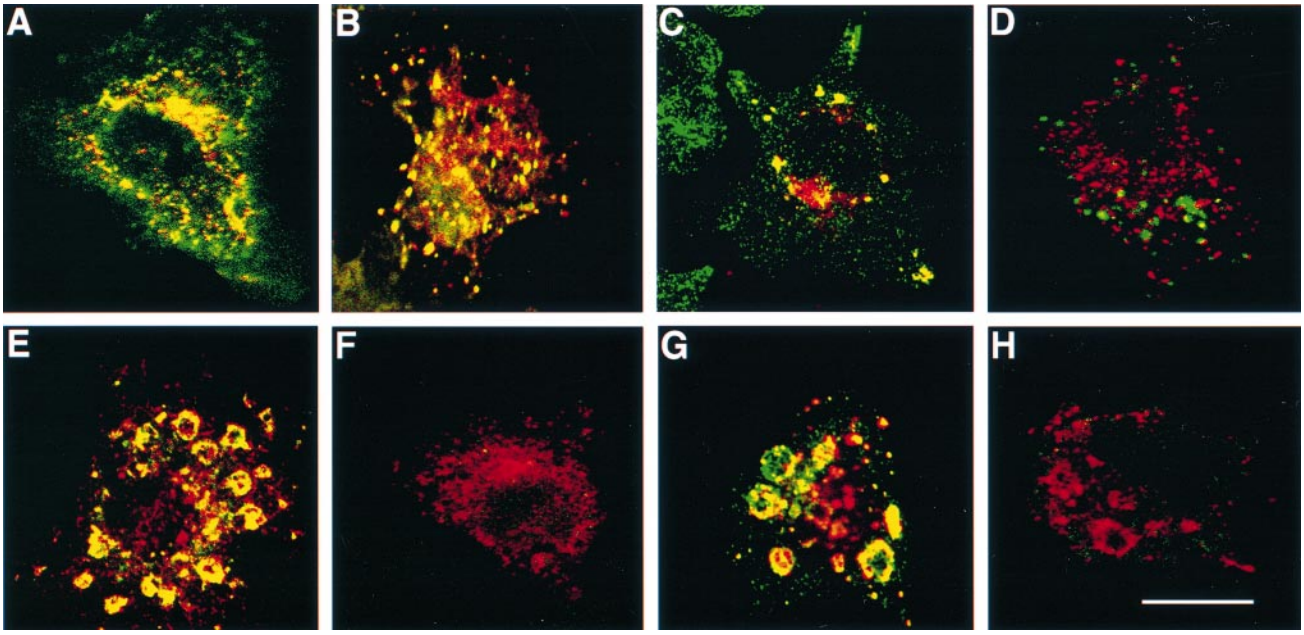

Fig. 7. Confocal immunofluorescence analysis of BHK cells co-expressing VSV-G::Rab5^{Q79L}, VSV-G::Rab4^{Q67L} or Rab7 with *myc*::Rabaptin-5 or various *myc*::Rabaptin-5 C- and N-terminal deletions. (**A**) Cells co-transfected with VSV-G::Rab4^{Q67L} and hTfR. (**B**) Cells co-transfected with VSV-G::Rab4^{Q67L} and full-length *myc*::Rabaptin-5. (**C**) Cells co-transfected with VSV-G::Rab4^{Q67L} and full-length *myc*::Rabaptin-5, and stained for VSV-G::Rab4 (red) and endogenous Rab5 (green). (**D**) Cells co-transfected with Rab7 and full-length *myc*::Rabaptin-5. (**E**) Cells co-transfected with VSV-G::Rab4^{Q67L} and *myc*::Rab5^{Q79L}. (**F**) Cells co-transfected with VSV-G::Rab4^{Q67L} and *myc*::Rabaptin-5 Δ547–862. (**G**) Cells co-transfected with VSV-G::Rab5^{Q79L} and *myc*::L1_46 (*myc*::Rabaptin-5 Δ1–550). (**H**) Cells co-transfected with VSV-G::Rab5^{Q79L} and *myc*::Rabaptin-5 Δ547–862. The cells were permeabilized with saponin prior to fixation and were stained with affinity purified rabbit anti-VSV-G polyclonal (A–C and E–H), affinity-purified rabbit anti-Rab7 polyclonal (D), affinity purified rabbit anti-Rab5 polyclonal (C), mouse anti-TfR B3/25 monoclonal (A) and/or mouse anti-*myc* 9E10 monoclonal (B–H) antibodies. Green indicates FITC anti-mouse secondary antibodies staining, except in (C) where an FITC anti-rabbit secondary antibody was used for endogenous Rab5 staining, whereas red represents Rhodamine anti-rabbit secondary antibodies staining (for Rab proteins). Overlays are shown with yellow indicating co-localization. Coverslips were viewed with the confocal microscope developed at EMBL, as described previously (Bucci *et al.*, 1992).

The early endosome is a highly dynamic and critical sorting station of the endocytic pathway (Gruenberg and Maxfield, 1995; Mellman, 1996). Vesicles derived from the plasma membrane deliver their cargo into early endosomes. From early endosomes, membrane proteins and solutes can either return to the surface via vesicular carriers or recycling tubules, or be transported to late endosomes and lysosomes. In addition, early endosomes are linked by transport routes to peri-nuclear recycling endosomes and to the biosynthetic pathway via the *trans*-Golgi network (TGN). To maintain the correct homeostasis of this plastic compartment which can also fuse homotypically *in vitro* and presumably *in vivo* (Gruenberg and Maxfield, 1995), membrane flow in and out of early endosomes must be coordinated. Two simple mechanisms can be envisaged for this regulation. One possibility is that the components that regulate the production and consumption of endocytic and recycling vesicles are rate-limiting. For example, overexpression of Rab5 alone stimulates endocytosis and endosome fusion *in vivo*, suggesting that this GTPase is expressed in limiting amount to regulate the kinetics of transport into early endosomes (Bucci *et al.*, 1992). An additional possibility is the existence of regulatory molecules which are shared and link sequential transport events. Based on our results, we propose that Rabaptin-5 could fulfil this role by acting as a molecular bridge between endocytosis and recycling, through the binding to the active forms of Rab5 and Rab4. This model implies that Rabaptin-5 would not be recruited by the two GTPases and function independently, but rather would be subjected to a sequential regulation, for example depending upon GTP-hydrolysis by Rab5. Two observations are consistent with this hypothesis. First, we did not observe efficient membrane recruitment of Rabaptin-5 C-terminal deletions containing the R4BD which were otherwise shown to interact with Rab4 in the yeast two-hybrid system. It is possible, therefore, that Rabaptin-5 is first recruited by Rab5 on the membrane and only subsequently interacts with Rab4. The interaction observed with Rab5 and Rab4 does not exclude the possibility that upon membrane recruitment by GTP-bound Rab5, Rabaptin-5 could additionally interact with other membrane-bound molecules which participate in vesicle docking and fusion, such as SNAREs. Secondly, the observation that overexpression of the GTPase-deficient Rab5^{Q79L} mutant not only increases the rate of transferrin internalization, but also inhibits its recycling (Stenmark *et al.*, 1994a), is consistent with the proposed role for Rabaptin-5 as a Rab5/Rab4 functional linker. By sequestering Rabaptin-5, the mutant Rab5 might either prevent the interaction with Rab4 or immobilize Rab4 in the expanded early endosomes (consistent with the immunofluorescence results of Figure 7), impeding its function in membrane recycling.

In order to test this model experimentally it is necessary to demonstrate that Rabaptin-5 indeed participates in the Rab4-dependent recycling step and that its activity depends on GTP-hydrolysis by Rab5. This will require the development of an *in vitro* assay that reconstitutes receptor recycling through the early endosomes. Our data do not necessarily exclude the involvement of other Rab4

effectors which would function in regulating transport along the recycling pathway. In coupling Rab5 to Rab4, Rabaptin-5 may regulate a rate-limiting step in this process. Our present observations describe a novel type of structural organization for a Rab protein effector which may provide insights into how bi-directional traffic of vesicles is coordinated at the molecular level.

Materials and methods

Plasmids

pHAT–UEP, pGEM–*myc*::L1_46, pGEM–Rab5^{Q79L}, pGEM–hTfR, pGADGH–L1_46, pLexA–Rab4b, pLexA–Rab5, pLexA–Rab5^{Q79L}, pLexA–Rab17 and pLexA–Rab22 have been described previously (Stenmark *et al.*, 1995b), as well as pGEM–Rab7 (Chavrier *et al.*, 1990). pLexA–Rab7 was from C.Bucci, the pLexA–Rab6 constructs were from I.Janoueix-Lerosey and B.Goud, and the pLexA–rasG12V and pLexA–laminC constructs were from A.Vojtek (Vojtek *et al.*, 1993). pLexA–Rab3a and pLexA–Rab3b constructs were obtained by cloning the respective cDNAs (kindly provided by R.Regazzi) into the polylinker sites of pBTM116 (Vojtek *et al.*, 1993). pLexA–Rab4a was obtained by cloning the cDNA (Touchot *et al.*, 1987) into the polylinker sites of pBTM116. pLexA–Rab4a was constructed by PCR amplification of Rab4a in pUC8 utilizing Rab4a–ATG plus *Bam*HI primer (5′-ACTAGTGCGGATCCTCCGAAACCTACGATTTTTTGT-3′) with the pUC 8 primer (5′-GTGCCAAGCTTGGCTGC-3′). Rab4a^{Q67L} was constructed by two-stage PCR amplification of Rab4a, using Rab4a in pUC 8 as a template with the primer Rab4a–ATG plus *Bam*HI (5′-ACTAGTGCGGATCCTCCGAAACCTACGATTTTTTGT-3′) and the primer Rab4a^{Q67L} (5′-GAATCGTTCGAGTCCTGCTGTATCCC-3′) creating the mutation. This first-round PCR product was then used as a primer together with a pUC 8-specific downstream primer (5′-GTGCCAAGCTTGGCTGC-3′) and the full-length Rab4a^{Q67L} PCR product was cloned into the *Bam*HI site of pBTM116 (pLexA). A similar strategy was used for the Rab4b^{Q67L} allele and the PCR product was cloned in pBTM116. Rab11^{Q70L} was subcloned in pBTM116 from pGEM–Rab11^{Q70L} (Ullrich *et al.*, 1996). pLexA–CC and pGADGH–CC were constructed by PCR amplification of corresponding Rabaptin-5 cDNA fragments. pGEM–*myc*UEP (*myc*-tagged Rabaptin-5) was obtained inserting the UEP*myc*-s (5′-CATGGCCCATATGGAACAAAAACTCATCTCAGAAGAGGATCTGGGCC-3′) and UEP*myc*-as (5′-CAGATCCTCTTCTGAGATGAGTTTTTGTTCCATATGGGC-3′) annealed oligos into *Nco*I/*Bsp*120I digested pGEM–UEP. pGEM-*myc*UEP Δ547–862 was obtained by *Eco*RI digestion and self-religating of pGEM–*myc*UEP after fill-in with Klenow enzyme; this realizes a frame shift and the creation of a stop codon 5 amino acids downstream of position 547 of Rabaptin-5. pGEM–GFP was obtained by PCR cloning of the GFP cDNA from pGFP10.1 (Chalfie *et al.*, 1994) using the GFP-A (5′-CGGAATTCCAGTAAAGGAGAAGAACTT-3′) and the GFP-B (5′-CGGGATCCCGGGGCCTGAATTTAACCAGGA-3′) primers in pGEM1. pGEM–GFP::Rabaptin 551–862, pGEM–GFP::Rabaptin 739–862, pGEM–GFP::Rabaptin 789–862 and pGEM–GFP::Rabaptin 807–862 were derived from pGEM–GFP by PCR cloning of the indicated Rabaptin-5 fragments at the 3′ of GFP. pGEM–GFP::Rabaptin 789–832 was obtained by digestion with *Bam*HI and self-religation of pGEM–GFP::Rabaptin 789–862 after fill-in with Klenow enzyme; this realizes a frame shift and the creation of a stop codon 6 amino acids downstream position 832 of Rabaptin-5. pGADGH–*myc*UEP, pGADGH–*myc*UEP Δ547–862, pGAD10–*myc*UEP, pGAD10–*myc*UEP Δ547–862 and pGAD10-L1_46 were obtained by subcloning corresponding fragments from the described pGEM constructs in pGADGH and pGAD10 (Clontech). pGAD10–*myc*UEP 5–235 and pGAD10–*myc*UEP 1–214 were derived from pGAD10–*myc*UEP digested with *Xba*I and *Stu*I, respectively, filled-in (*Xba*I), and religated in presence of a *Spe*I-ter self-annealed oligo (5′-CTAGACTAGTCTAG-3′), thus introducing a stop codon at the site of insertion. pGAD10–*myc*UEP 5–135 and pGAD10–*myc*UEP 135–214 were constructed by PCR amplification of corresponding *myc*::Rabaptin-5 cDNA fragments. pGADGH–Rabaptin 739–862, pGADGH–Rabaptin 789–862 and pGADGH–Rabaptin 809–862 were obtained by PCR cloning of the indicated Rabaptin-5 fragments in pGADGH. pGADGH–Rabaptin 789–832 was derived from pGADGH–Rabaptin 789–862 which was *Bam*HI-digested, filled-in and self-religated. The L1_46 Δ809–832 allele was created by oligonucleotide mutagenesis and subsequently cloned in pGADGH. pGEMVSVG was obtained by cloning the annealed VSV-G A and B oligos (A: 5′-CATGGCCCATATGTACACCGACATCGAGATGAACCGCCTGGGCAAGTCAATTG-3′) (B: 5′-AATTCAATTGACTTGCCCAGGCGGTTCATCTCGATGTCGGTGTACATATGGGC-3′) in pGEM1. pGEMVSVG–Rab4a^{Q67L} and pGEMVSVG–Rab5^{Q79L} were obtained by subcloning *Eco*RI/*Pst*I fragments from the corresponding pLexA constructs into pGEMVSVG. pMALc2–Rab4a and pMALc2–Rab6 were obtained by subcloning *Eco*RI/*Pst*I fragments from the corresponding pLexA constructs into pMALc2 (Biolabs).

Yeast two-hybrid methods

The yeast reporter strain L40 [Vojtek *et al.*, 1993; MATa his3D200 trp1–901 leu2–3112 ade2 LYS2:: (lexA–*HIS3*) (URA3::lexA–*lacZ*) GAL4] was co-transformed with the indicated 2μ/TRP1 pLexA and 2μ/LEU2 pGAD plasmids using a lithium acetate-based method (Schiestl and Giest, 1989) and the transformants were selected on synthetic defined complete (SDC) medium lacking tryptophan and leucine. *HIS3* reporter gene activation analysis was performed spotting 10 μl of an overnight culture (OD_{600} = 1) 1:50 dilution, on SDC medium lacking tryptophan, leucine and histidine. Liquid β-Gal assays for reporter *lacZ* gene activation analysis were performed as described previously (Stenmark *et al.*, 1995b). All yeast media were purchased from Bio101.

Cells and transfection

BHK-21 cells were grown in Glasgow's minimal essential medium containing 10% tryptose phosphate broth (Gibco-BRL) and 5% fetal calf serum (Gibco-BRL). HeLa cells were grown in Eagle's minimal essential medium containing 10% fetal calf serum. For overexpression studies, BHK-21 or HeLa cells were infected for 30 min with T7 RNA polymerase recombinant vaccinia virus (vT7) and then transfected with plasmids containing the cDNA of interest, using DOTAP (Boehringer Mannheim) as described previously (Stenmark *et al.*, 1995a). The cells were analysed 5 h post-transfection.

Antibodies

Rabbit polyclonal affinity purified anti-Rab7 and anti-Rabaptin-5 antibodies have been described previously (Chavrier *et al.*, 1991; Stenmark *et al.*, 1995b); rabbit polyclonal affinity purified anti-peptide (YTDIEMNRLGK) VSV-G epitope antibodies were a kind gift from Dr T.Nilsson. Monoclonal antibodies against the human Transferrin receptor (B3/25) and anti-*myc* epitope (9E10) were purchased from Boehringer Mannheim.

Confocal immunofluorescence microscopy

Cells on 11 mm round glass coverslips were fixed with 3% paraformaldehyde. HeLa cells expressing GFP and GFP::Rabaptin-5 fusions were mounted directly on Mowiol (Hoechst) without any further treatment and examined in the confocal microscope. BHK cells were permeabilized with 0.05% saponin (Sigma) prior to fixation. Free aldehyde groups were quenched with 50 mM NH_4Cl, and the fixed cells were incubated with primary antibodies, as described previously (Stenmark *et al.*, 1995a). Secondary antibodies were rhodamine donkey anti-rabbit and FITC-conjugated donkey anti- mouse IgG (Jackson Immunoresearch). Coverslips were mounted on Mowiol and examined by confocal microscopy at excitation wavelengths of 476 and 529 nm.

Recombinant proteins

BL-21 (DE3) *Escherichia coli* cells transformed with pHAT–UEP (Stenmark *et al.*, 1995b) were incubated for 3 h at 37°C in the presence of 0.3 mM IPTG, in order to induce expression of the His_6-tagged proteins. His-tagged Rabaptin-5 was purified on Ni^{2+} agarose (Qiagen), according to the native purification protocol from the manufacturer, followed by gel-filtration chromatography on Superose-12 column (Pharmacia). By this purification, His_6::Rabaptin-5 was >95% pure. MBP::Rab4 and MBP::Rab6 were expressed from XL1blue *E.coli* cells (Stratagene) transformed with pMAL–Rab4 and pMAL–Rab6, and purified using amylose resin (Biolabs) according to the manufacturer's protocol, with the exception that 10 μM GDP and 2 mM $MgCl_2$ were added in the column buffer. By this purification MBP::Rab4 and MBP::Rab6 were >80% pure.

In vitro binding studies with recombinant proteins

MBP–Rab4 and MBP–Rab6 were immobilized on Affi-Gel 15 beads according to manufacturer's instructions (Bio-Rad). The amount of protein bound to the beads (~25 μg:50 μl of beads) was verified by protein assay (Bio-Rad) subtracting the amount inputted with the flow-through fractions; typically 95% of the input was bound to the beads.

Then, each sample was divided into three aliquots, washed and incubated in low Mg^{2+} concentration buffer (20 mM HEPES, pH 7.5, 100 mM NaCl, 1 mM DTT, 10 mM EDTA, 5 mM $MgCl_2$) containing 100 μM of the appropriate nucleotide (GDP or GTPγS) or no nucleotide (free form) at room temperature for 1 h under rotation, in order to obtain nucleotide exchange. The beads were washed and incubated with stabilization buffer (20 mM HEPES, pH 7.5, 100 mM NaCl, 1 mM DTT, 2 mM $MgCl_2$) containing 100 μM of the appropriate nucleotide for 10 min at room temperature under rotation. Subsequently, the different nucleotide forms of MBP::Rab4 and MBP::Rab6 were incubated with a 40% ammonium sulfate-precipitated bovine brain cytosol fraction (0.2 mg), dialysed against buffer A (20 mM HEPES/KOH, pH 7.2, 5 mM $MgCl_2$, 1 mM DTT), or with recombinant Rabaptin-5 (5 μg) for 1 h at 4°C. The beads were then washed six times for 30 min with stabilization buffer containing 10 μM of the appropriate nucleotide. Finally, proteins bound on the beads were analysed by SDS–PAGE followed by immunoblotting using anti-Rabaptin-5 antibodies and enhanced chemiluminesence (ECL) as the detection method.

Preparation of cytosol

Bovine brain cytosol was prepared from fresh bovine brain homogenate in BHB buffer (50 mM KCl, 50 mM HEPES, 10 mM EGTA, 2 mM $MgCl_2$, pH 7.4, KOH) which was first centrifuged at 4200 *g* at 4°C for 15 min; the resulting post-nuclear supernatant was then centrifuged at 100 000 *g* at 4°C for 60 min, in order to pellet the membranes and obtain a cytosolic fraction with a typical total protein concentration of 20–30 mg/ml. HeLa cytosol was prepared as described previously (Stenmark *et al.*, 1995b) and had a total protein concentration of ~5 mg/ml.

Cross-linking of cytosolic and recombinant Rabaptin-5

One hundred μl of HeLa cytosol or 0.1 μM recombinant Rabaptin5 were incubated with the indicated concentrations of the covalent cross-linker BS^3 (Pierce) in phosphate-buffered saline (0.1 M phosphate, 0.15 M NaCl, pH 7.2) for 30 min at 30°C. Free reactive groups were then quenched in 0.2 M Tris–Cl (pH 7) on ice for 30 min. Finally, the reactions were analysed by SDS–PAGE and subsequent immunoblot using anti-Rabaptin-5 antibodies and enhanced chemiluminesence (ECL) as the detection method.

CD analysis of recombinant Rabaptin-5

CD spectra were recorded on JASCO-710 dichrograph calibrated with (1s)-(+)-10-camphorsulfonic acid. The sample was in 10 mM phosphate buffer pH 7.2, 0.5 mM 2-mercaptoethanol and 1 μM His_6::Rabaptin-5. Single scans in the range of 180–250 nm were obtained at the temperature of 293 K with 0.2 nm intervals, 1 s integration time and 1 mm slit width. A 0.1 cm path length cell was used for the analysis. The spectrum is the average of 30 scans smoothed by using the reverse Fourier transform noise reduction software from JASCO, after baseline subtraction. The helical content of Rabaptin-5 was estimated using the empirical equation developed by Cheng *et al.* (1974): $\%\text{helix} = 100\{\theta_{222}/[-39500(1-2.57/n)]\}$ where θ_{222} is the ellipticity of the protein at 222 nm and *n* is the number of peptides bound.

Fractionation of Rabaptin-5

Analysis of recombinant and native Rabaptin-5 by size exclusion chromatography and density gradient centrifugation was carried out as described (Horiuchi *et al.*, 1997). For the co-fractionation studies shown in Figure 6C, 10 μM His-tagged Rab4 and Rab5 were pre-loaded with GDP or GTPγS (Horiuchi *et al.*, 1997) and incubated in the presence of 4 μM recombinant His-tagged Rabaptin-5 in 20 mM HEPES, 2 mM $MgCl_2$, 1 mM DTT, 100 mM NaCl, pH 7.4, KOH for 10 min at 30°C. The reaction mixture was centrifuged and loaded on a Superdex 200 PC 3.2/30 column (Pharmacia) equilibrated with the same buffer. The chromatographic separation was carried out in a SMART system (Pharmacia). Fractions of 60 μl were collected beginning from 600 μl eluate and analysed by SDS–PAGE and Western blot, using anti-Rab5, -Rab4 and -Rabaptin-5 antibodies.

Acknowledgements

We are grateful to Cecilia Bucci, Romano Regazzi and Tommy Nilson for generous gifts of reagents, to Jamie White and Sigrid Reinsch for help in confocal microscopy analysis and to Angelika Giner and Eva Rønning for superb technical assistance and help in various experiments. We thank Roger Lippé, Heidi McBride and Eric Nielsen for critical reading of the manuscript. This work was supported by grants from the Human Frontier Science Program (RG-432/96), EC HCM and TMR Grants (ERB-CT94-0592 and ERB-CT96-0020) (M.Z., H.S. and M.McC.) and the Norwegian Cancer Society and by the Novo Nordisk Foundation (H.S.).

References

Berger,B., Wilson,D.B., Wolf,E., Tonchev,T., Milla,M. and Kim,P.S. (1995) Predicting coiled coils by use of pairwise residue correlations. *Proc. Natl Acad. Sci. USA*, **92**, 8259–8263.

Bucci,C., Parton,R.G., Mather,I.H., Stunnenberg,H., Simons,K., Hoflack,B. and Zerial,M. (1992) The small GTPase rab5 functions as a regulatory factor in the early endocytic pathway. *Cell*, **70**, 715–728.

Chalfie,M., Tu,Y., Euskirchen,G., Ward,W.W. and Prasher,D.C. (1994) Green fluorescent protein as a marker for gene expression. *Science*, **263**, 802–805.

Chavrier,P., Parton,R.G., Hauri,H.P., Simons,K. and Zerial,M. (1990) Localization of low molecular weight GTP binding proteins to exocytic and endocytic compartments. *Cell*, **62**, 317–329.

Chavrier,P., Gorvel,J.P., Steltzer,E., Simons,K., Gruenberg,J. and Zerial,M. (1991) Hypervariable C-terminal domain of rab proteins acts as a targeting signal. *Nature*, **353**, 769–772.

Cheng,Y.H., Yang,J.T. and Chan,K.H. (1974) Determination of the helix and b form of proteins in aqueous solution by circular dichroism. *Biochemistry*, **13**, 3350–3359.

Cosulich,S.C., Horiuchi,H., Zerial,M., Clarke,P.R. and Woodman,P.G. (1997) Cleavage of Rabaptin-5 blocks endosome fusion during apoptosis. *EMBO J.*, **16**, 6182–6191.

Daro,E.P., van der Sluijs,P., Galli,T. and Mellman,I. (1996) Rab4 and cellubrevin define different early endosome populations on the pathway of transferrin receptor recycling. *Proc. Natl Acad. Sci. USA*, **93**, 9559–9564.

Ghosh,R.N., Gelman,D.L. and Maxfield,F.R. (1994) Quantification of low-density lipoprotein and transferrin endocytic sorting in Hep2 cells. *J. Cell Biol.*, **128**, 549–561.

Gournier,H., Stenmark,H., Rybin,V., Lippé,R. and Zerial,M. (1998) Two distinct effectors of the small GTPase Rab5 cooperate in endocytic membrane fusion. *EMBO J.*, **17**, 1930–1940.

Gruenberg,J. and Maxfield,F.R. (1995) Membrane transport in the endocytic pathway. *Curr. Opin. Cell Biol.*, **7**, 552–563.

Guarente,L. (1983) Yeast promoters and *lacZ* fusions designed to study expression of cloned genes in yeast. *Methods Enzymol.*, **101**, 181–189.

Harrington,W.F. and Rodgers,E. (1984) Myosin. *Annu. Rev. Biochem.*, **53**, 35–73.

Heitlinger,E., Peter,M., Haner,M., Lustig,A., Aebi,U. and Nigg,E.A. (1991) Expression of chicken lamin B2 in *Escherichia coli*: characterization of its structure, assembly, and molecular interactions. *J. Cell Biol.*, **113**, 485–495.

Hopkins,C.R., Gibson,A., Shipman,M., Strickland,D.K.a. and Trowbridge,I.S. (1994) In migrating fibroblasts, recycling receptors are concentrated in narrow tubules in the pericentriolar area, and then routed to the plasma membrane of the leading lamella. *J. Cell Biol.*, **125**, 1265–1274.

Horiuchi,H. *et al.* (1997) A novel Rab5 GDP/GTP exchange factor complexed to Rabaptin-5 links nucleotide exchange to effector recruitment and function. *Cell*, **90**, 1149–1159.

Joshua,G.W. and Hsieh,C.Y. (1995) Stage-specifically expressed genes of *Angiostrongylus cantonensis*: identification by differential display. *Mol. Biochem. Parasitol.*, **71**, 285–289.

Lombardi,D., Soldati,T., Riederer,M.A., Goda,Y., Zerial,M. and Pfeffer,S.F. (1993) Rab9 functions in transport between late endosomes and the trans Golgi network. *EMBO J.*, **12**, 677–682.

Lupas,A. (1996) Coiled coils: new structures and new functions. *Trends Biochem. Sci.*, **21**, 375–382.

Lütcke,A., Jansson,S., Parton,R.G., Chavrier,P., Valencia,A., Huber,L., Lehtonen,E. and Zerial,M. (1993) Rab17, a novel small GTPase, is specific for epithelial cells and is induced during cell polarization. *J. Cell Biol.*, **121**, 553–564.

McKeon,F.D., Kirschner,M.W. and Caput,D. (1986) Homologies in both primary and secondary structure between nuclear envelope and intermediate filament proteins. *Nature*, **319**, 463–468.

Mellman,I. (1996) Endocytosis and molecular sorting. *Ann. Rev. Cell Dev. Biol.*, **12**, 575–625.

Novick,P. and Zerial,M. (1997) The diversity of Rab proteins in vesicle transport. *Curr. Opin. Cell Biol.*, **9**, 496–504.

Olkkonen,V.M., Dupree,P., Killisch,I., Lütcke,A., Zerial,M. and Simons,K. (1993) Molecular cloning and subcellular localization of three GTP-binding proteins of the Rab subfamily. *J. Cell Sci.*, **106**, 1249–1261.

Pfeffer,S.R. (1994) Rab GTPases: master regulators of membrane trafficking. *Curr. Opin. Cell Biol.*, **6**, 522–526.

Rothman,J.E. (1994) Mechanisms of intracellular protein transport. *Nature*, **372**, 55–63.

Rybin,V., Ullrich,O., Rubino,M., Alexandrov,K., Simon,I., Seabra,M.C., Goody,R. and Zerial,M. (1996) GTPase activity of rab5 acts as a timer for endocytic membrane fusion. *Nature*, **383**, 266–269.

Schiestl,R.H. and Giest,R.D. (1989) High efficiency transformation of intact cells using single stranded nucleic acids as a carrier. *Curr. Genet.*, **16**, 339–346.

Stenmark,H., Parton,R.G., Steele-Mortimer,O., Lütcke,A., Gruenberg,J. and Zerial,M. (1994a) Inhibition of rab5 GTPase activity stimulates membrane fusion in endocytosis. *EMBO J.*, **13**, 1287–1296.

Stenmark,H., Valencia,A., Martinez,O., Ullrich,O., Goud,B. and Zerial,M. (1994b) Distinct structural elements of rab5 define its functional specificity. *EMBO J.*, **13**, 575–583.

Stenmark,H., Bucci,C. and Zerial,M. (1995a) Expression of Rab GTPases using recombinant vaccinia virus. *Methods Enzymol.*, **257**, 155–164.

Stenmark,H., Vitale,G., Ullrich,O. and Zerial,M. (1995b) Rabaptin-5 is a direct effector of the small GTPase Rab5 in endocytic membrane fusion. *Cell*, **83**, 423–432.

Touchot,N., Chardin,P. and Tavitian,A. (1987) Four additional members of the ras gene superfamily isolated by an oligonucleotide strategy: molecular cloning of YPT-related cDNAs from a rat brain library. *Proc. Natl Acad. Sci. USA*, **84**, 8210–8214.

Ullrich,O., Reinsch,S., Urbé,S., Zerial,M. and Parton,R.G. (1996) Rab11 regulates recycling through the pericentriolar recycling endosome. *J. Cell Biol.*, **135**, 913–924.

van der Sluijs,P., Hull,M., Zahraouri,A., Tavitian,A., Goud,B. and Mellman,I. (1991) The small GTP-binding protein rab4 is associated with early endosomes. *Proc. Natl Acad. Sci. USA*, **88**, 6313–6317.

van der Sluijs,P., Hull,M., Webster,P., Mâle,P., Goud,B. and Mellman,I. (1992) The small GTP-binding protein rab4 controls an early sorting event on the endocytic pathway. *Cell*, **70**, 729–740.

Vojtek,A.B., Hollenberg,S.M. and Cooper,J.A. (1993) Mammalian Ras interacts directly with the serine/threonine kinase Raf. *Cell*, **74**, 205–214.

Yamashiro,D.J. and Maxfield,F.R. (1984) Segregation of transferrin to a mildly acidic (pH 6.5) para-Golgi compartment in the recycling pathway. *Cell*, **37**, 389–400.

Received October 22, 1997; revised and accepted February 6, 1998